Supporting material to

Recent past (1979-2014) and future (2070-2099) isoprene fluxes over Europe simulated with the MEGAN-MOHYCAN model

Maite Bauwens[1], Trissevgeni Stavrakou[1], Jean-François Müller[1], Bert Van Schaeybroeck[2], Lesley De Cruz[2], Rozemien De Troch[2], Olivier Giot[2,3], Rafiq Hamdi[2], Piet Termonia[2], Quentin Laffineur[2], Crist Amelynck[1], Niels Schoon[1], Bernard Heinesch[4], Thomas Holst[5], Almut Arneth[6], Reinhart Ceulemans[3], Arturo Sanchez-Lorenzo[7], Alex Guenther[8]

[1] Royal Belgian Institute for Space Aeronomy, Avenue Circulaire 3, 1180, Brussels, Belgium

[2] Royal Meteorological Institute, Avenue Circulaire 3, 1180, Brussels, Belgium

[3] Centre of Excellence PLECO (Plant and Vegetation Ecology), Department of Biology, University of Antwerp, 2610 Wilrijk, Belgium

[4] Gembloux Agro-Bio Tech, University of Liège, Unité de Physique des Biosystèmes, Avenue de la Faculté d'Agronomie 8, 5030 Gembloux, Belgium

[5] Department of Physical Geography and Ecosystems Analysis, Lund University, Sweden

[6] Karlsruhe Institute of Technology, Institute of Meteorology and Climate Research, Atmospheric Environmental Research (IMK-IFU), Garmisch-Partenkirchen, Germany

[7] Pyrenean institute of Ecology (IPE), Spanish National Research Council, Zaragoza, Spain

[8] Department of Earth System Science, University of California, Irvine, California 92697, USA

Manuscript submitted to

Biogeosciences

2017

This supplement contains 7 figures which support the main manuscript.
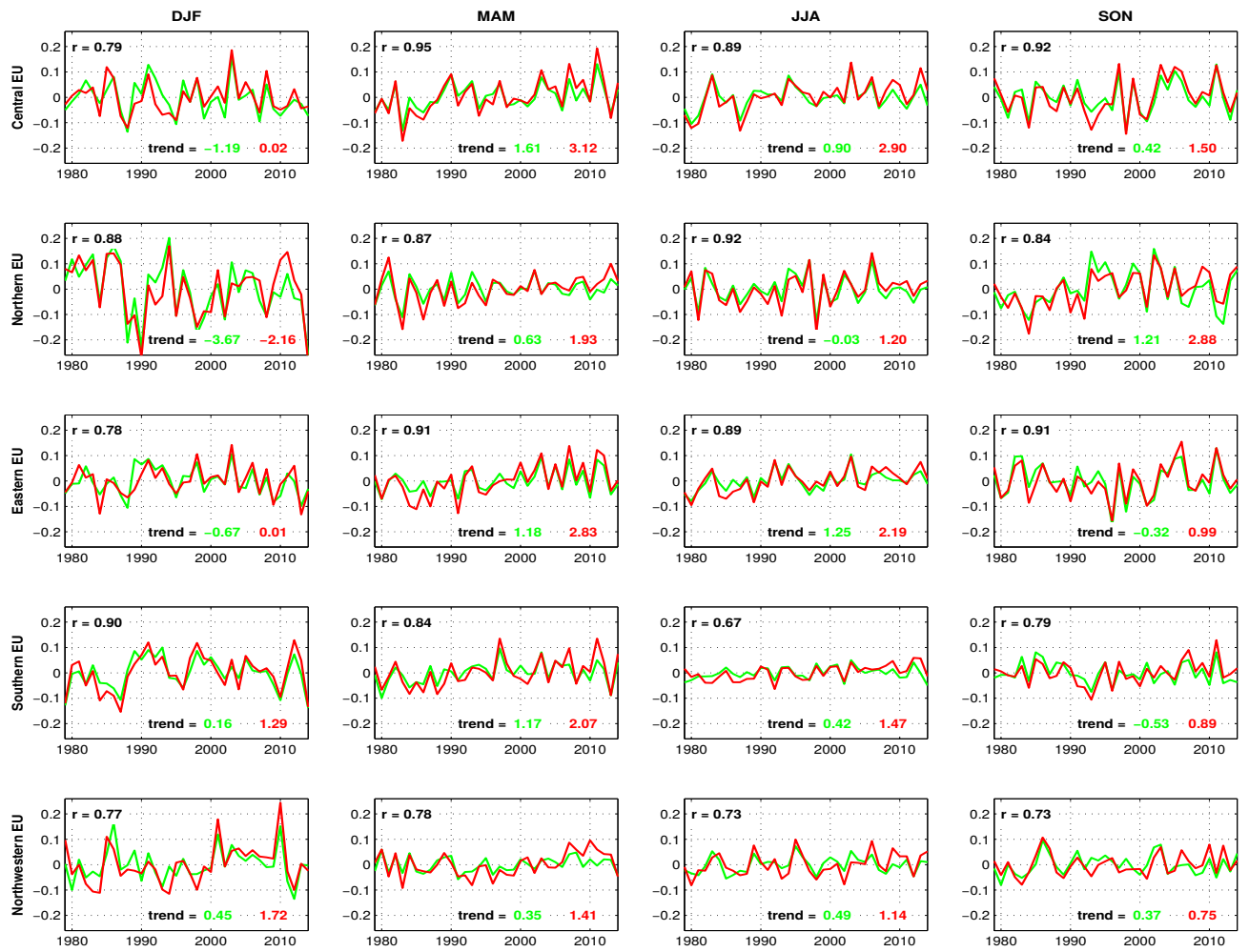
Figure S1. Seasonal surface solar radiation anomaly data according to the ECMWF model (green) and according to ground-based observations (red). The calculated decadal trends (%/decade) and correlation coefficients are inset. DJF: December-January-February; MAM: March-April-May; JJA: June-July-August; SON: September-October-November.
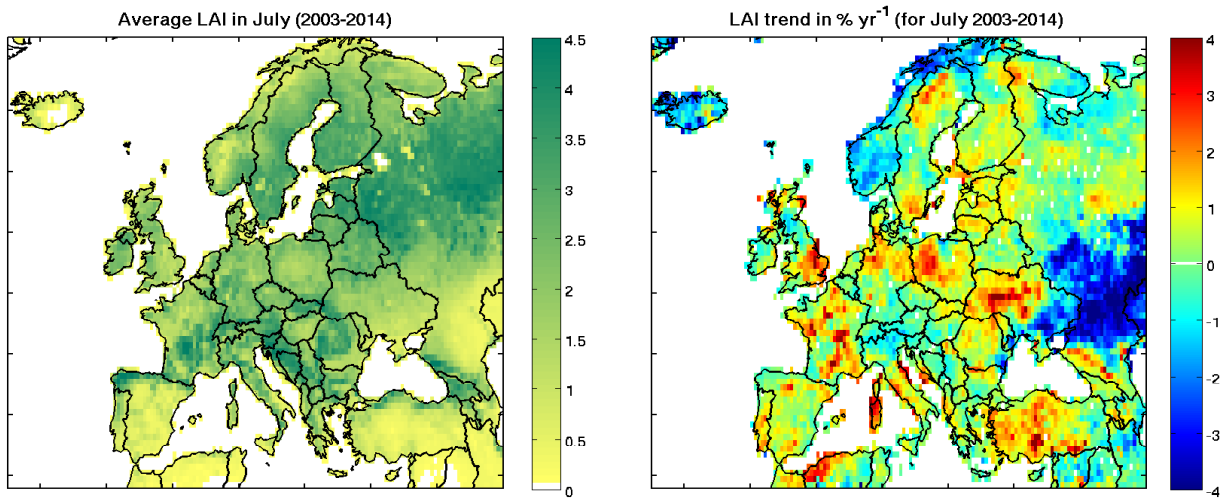
Figure S2. Distribution of average LAI over Europe in July averaged over 2003-2014, and the calculated LAI trend over this period.
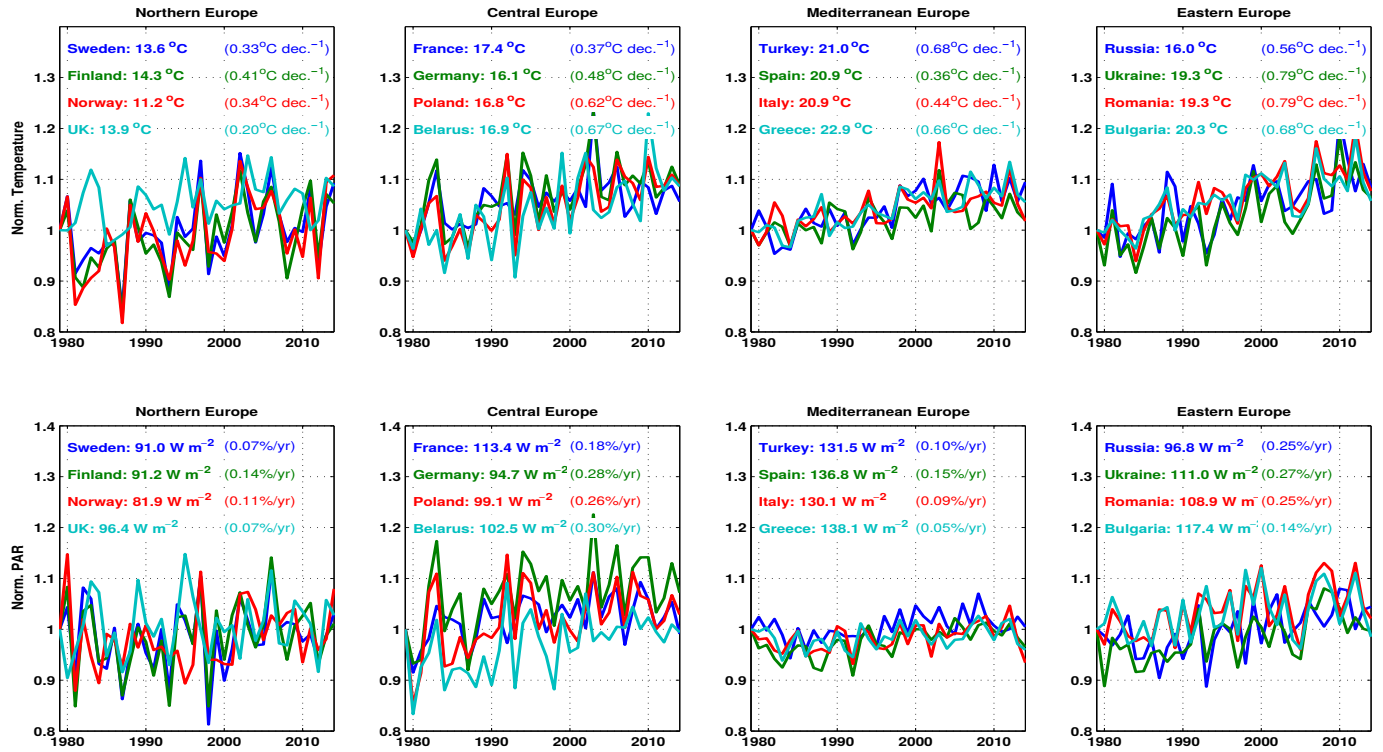
Figure S3. Interannual variability and trend in ERA-Interim ECMWF summer temperatures and solar radiation for 16 countries of northern, central, Mediterranean and eastern Europe. The data are normalized to their 1979 values, and the average for that year is given in the upper left corner.

Landscape heterogeneity: model versus local vegetation composition

Vegetation composition in the 0.1x0.1 grid cell   Local vegetation composition at study site

■ Needleleaf evergreen   ■ Needleleaf deciduous   ■ Broadleaf evergreen   ■ Broadleaf deciduous   ■ Shrub   ■ Crop   ■ Grass   ■ No vegetation
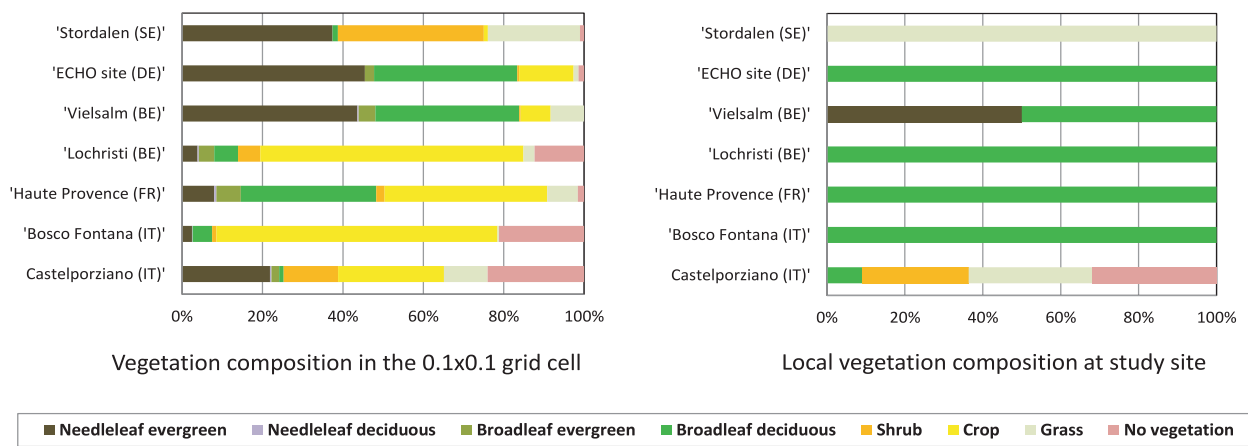
Figure S4. Landscape composition at the measurement sites shown in Fig. 4, as assumed in the model grid cell (left), and based on the corresponding literature studies (right). For sites where the precise percentages are not reported (e.g. Castelporziano), an assumption is made based on the site description as provided in the corresponding publication.
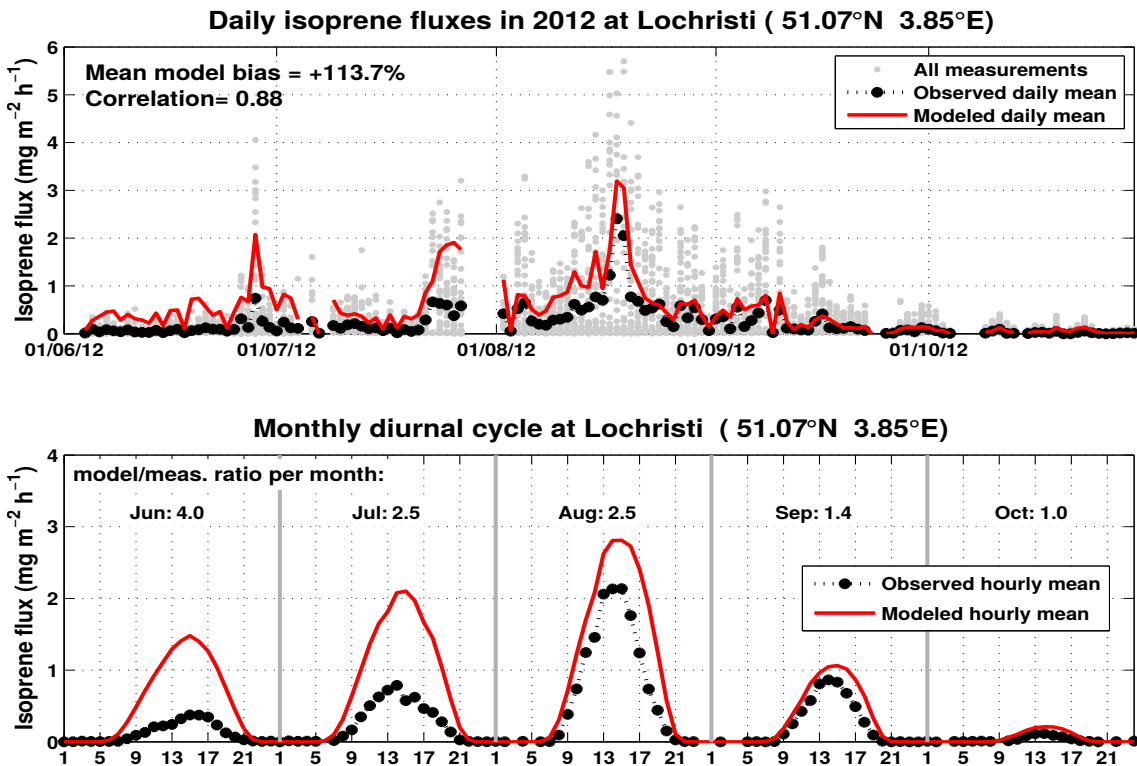
Figure S5. Upper panel : Modeled (red) and measured (black and gray) daily isoprene fluxes in Lochristi (Belgium) in 2012 (Brilli et al. 2014). The model (H3 simulation) uses the emission factor for broadleaf trees recommended in the MEGAN model ($10\ \mathrm{mg\ m^{-2}\ h^{-1}}$). Lower panel : monthly diurnal cycle for the modeled (red) and measured (black) isoprene fluxes. The monthly ratio of the model to the measured flux is given inset.

The ALARO regional climate model

 In Fig. S6 we compare the ALARO fields with the ERA-Interim fields over the control period 1976-2005 for temperature and shortwave solar radiation (Fig. S6). The average temperature of ALARO over land is estimated at 4.9°C for the full domain (34-70°N, 25°W-50°E), by 2.1°C lower than the average ECMWF temperature over 1979-2005. The cold bias of ALARO compared to ECMWF data reaches -6°C in mountainous regions and in northeastern Europe, but it does not exceed -2°C in central Europe. On the other hand, Fig. S6 shows a positive irradiance bias of ALARO compared to the ECMWF fields. The differences are strongest over Scandinavia, Russia and Turkey, whereas almost negligible or negative in western Europe.

 The use of the ALARO meteorology results in 35% lower mean isoprene emission over the European domain, i.e. 4.6 vs. 6.2 Tg/yr, with the strongest decrease (up to 90%), in southern Europe. The relatively low isoprene emission obtained over most parts of Europe using the ALARO meteorological fields are mostly due to the low temperature bias. Over Ukraine, Poland and Belarus isoprene emissions are ca. 20% higher in the ALARO simulation. In Scandinavia and over northern Russia the negative temperature bias is somewhat counteracted by the positive irradiance bias, resulting in a weak emission difference. Overall, the use of ALARO meteorology results in lower isoprene emissions compared to the H1-H3 estimates.

 Surface temperature, precipitation and surface shortwave radiation for the different RCP scenarios are compared to the control run in Fig. S7.
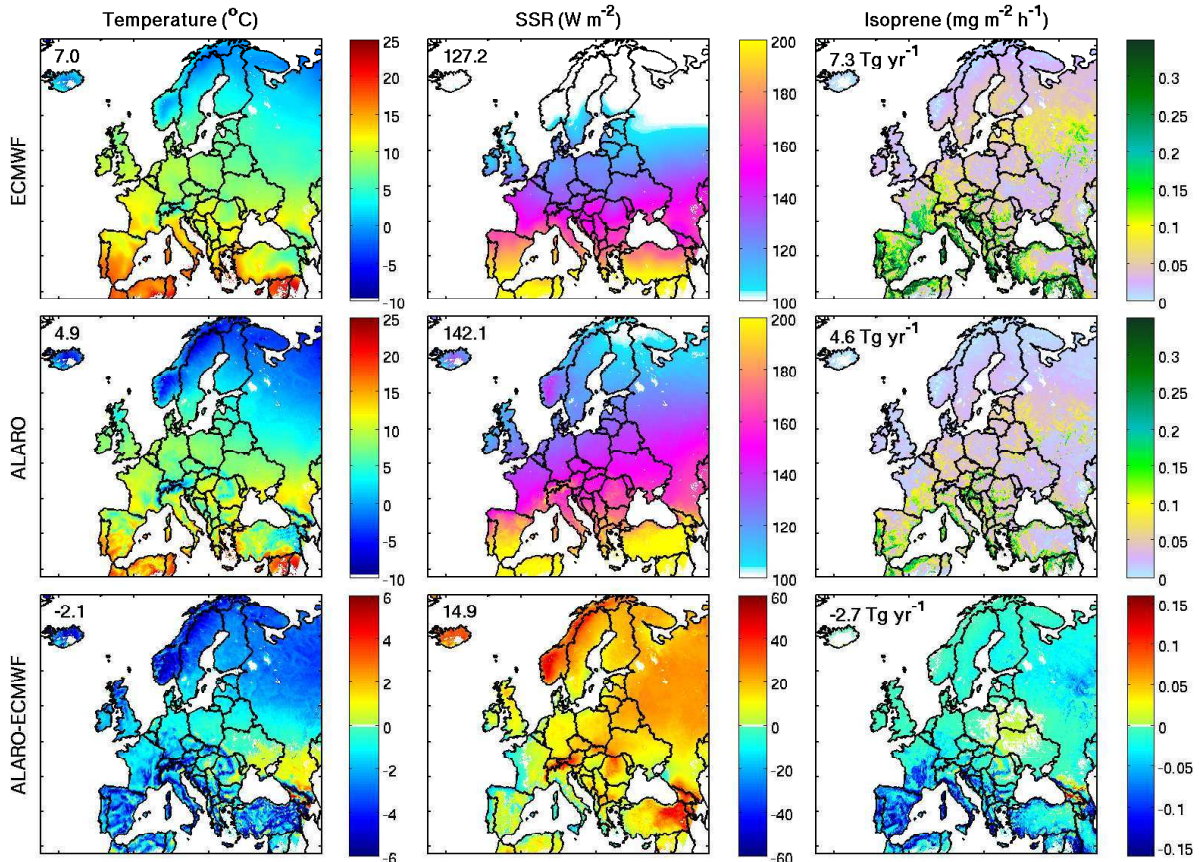
Figure S6. Mean annual temperature ($^{\circ}$C), irradiance (Wm^{-2}) and isoprene flux (mg m^{-2}h^{-1}) according to ERA-Interim ECMWF (upper panels) and ALARO (middle panels) meteorological fields. The lower panels show the absolute difference between the ALARO model and the ERA-Interim ECMWF data. The numbers inside the panels denote the domain average.
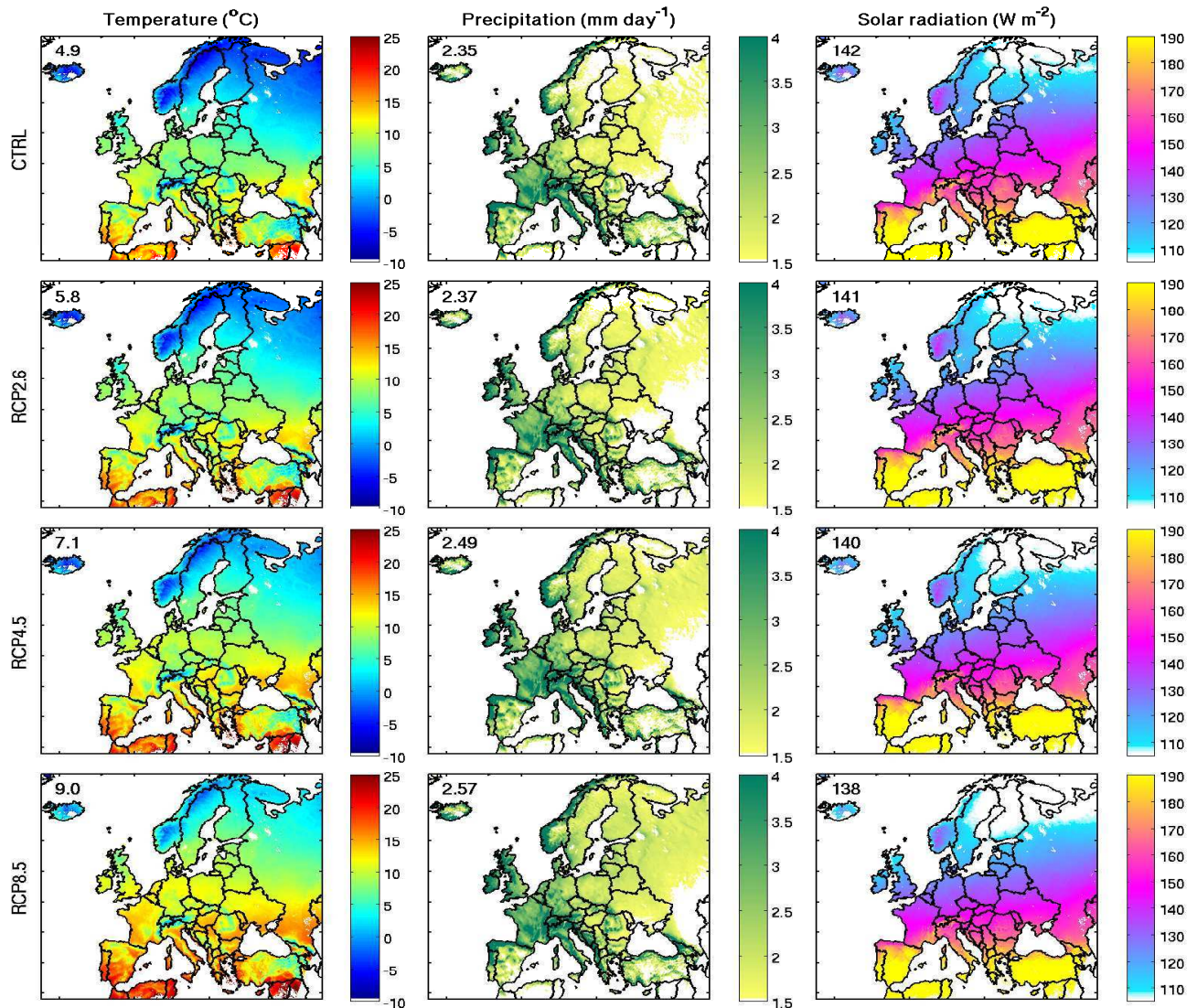
Figure S7. Surface temperature, precipitation and surface shortwave radiation for the different RCP scenarios, compared to the control run (Table 1). The corresponding means are given inside each panel.